2023 62nd IEEE Conference on Decision and Control (CDC)
December 13-15, 2023. Marina Bay Sands, Singapore

Singular Perturbation-Based Approach for Robust Control of Reluctance-Actuated Motion Systems

Mohammad Al Saaideh Almuatazbellah M. Boker Mohammad Al Janaideh

Abstract— **This paper introduces a new composite control approach for a motion system driven by a reluctance actuator. To achieve high-performance control, the method leverages singular perturbation theory to divide the problem into two components: a fast control problem and a slow control problem. A feedforward controller is developed based on the reduced system to address the fast control problem. The dynamic model is then formulated using the feedforward control law to address the slow control problem. Full-state feedback control chooses the input signal that results in the desired reference signal. The output signal of the feedback control is treated as the desired input for the feedforward controller. With the proposed approach, the feedforward controller for the fast dynamic eliminates the need for measuring the fast states. The effectiveness of the proposed approach is demonstrated through experimental testing.**

I. INTRODUCTION

Precision motion systems play a crucial role in meeting the demands of modern Micro/Nano-position applications [1]. Some examples of these systems include the wafer scanner in semiconductor manufacturing [2]. Electromagnetic actuators are widely developed and used to drive precision motion systems with a motion range of millimeters and micrometres [3]. Among them, reluctance actuators (RA) have been introduced as a solution for driving short-stroke motion stages, such as C-core and E-core reluctance actuators [4]–[6], hybrid-reluctance actuator [7], and plunger reluctance actuator [8]. Compared to other electromagnetic actuators, the RA offers relatively high force density and lower energy dissipation [9]. However, the application of this actuator is restricted in high-precision motion systems due to its high nonlinearity. These nonlinearities include the quadratic relation between the magnetic flux and magnetic, the air gap dependency [4], [5], and the magnetic hysteresis of the material [6].

In the last decade, several studies have been proposed to linearize the dynamic behavior of the RA. These studies aimed to develop a control system that compensates for the nonlinearities of the RA. Examples of such studies include feedforward compensation with inverse hysteresis model [6], observer-based on sheared-hysteresis model [5], and sensing coil voltage control circuitry with air gap observer [4]. These studies mainly focused on developing control systems for reluctance actuators at a constant air gap, overlooking the control systems required when incorporating the reluctance actuator into a motion system where the mover is part of the moving stage. Furthermore, the most proposed control approach for reluctance actuators requires the measurement of magnetic flux. In recent years, the hybrid-reluctance actuator has emerged in micropositioning. This actuator combines a reluctance actuator with an additional permanent magnet on the mover. Several studies have been conducted on this type of actuator, including [7], [10]. However, using permanent magnets in the hybrid design can lead to demagnetization effects, decreasing performance, output force, and efficiency over time. Moreover, the presence of permanent magnets can make the manufacturing process of the hybrid-reluctance actuator more challenging and costly compared to other reluctance actuators.

The singular perturbation approach is a mathematical technique that helps analyze the behavior of dynamic systems with two-time scales. One set of parameters is much larger than the other by scaling the system's parameters, effectively separating the system's fast and slow dynamics, which can be modeled separately [11]. This approach takes advantage of the fact that fast dynamics can be assumed to be in steady-state. In contrast, the slow dynamics evolve, simplifying complex systems and resulting in more accurate predictions of system behavior. Researchers have demonstrated the approach's effectiveness, showing improved control performance and accuracy in system behavior prediction, as seen in recent studies [12]–[14].

We have formulated a novel composite control approach for reluctance-actuated motion systems using the singular perturbation technique. We employ a feedforward controller to address the fast dynamic problem, while a full-state feedback controller is utilized to handle the slow dynamic problem. Initially, we reformulate the dynamic model of the system using the singular perturbation method by choosing a small constant. Next, we discuss the design process for our proposed composite control approach. Finally, we integrate an extended high-gain observer with the state feedback controller to resolve the output feedback control problem. The main contribution of the paper is summarized as

- Develop a robust control approach using singular perturbation that merges a feedforward controller with a state feedback controller. The feedforward controller provides an advantage as there is no requirement for

M. Al Saaideh is with the Department of Mechanical and Mechatronics Engineering, Memorial University, St. John's, NL A1B 3X5, Canada. mialsaaideh@mun.ca

A. M. Boker is with the Bradley Department of Electrical and Computer Engineering, Virginia Tech, Blacksburg, VA 24060, USA. boker@vt.edu

M. Al Janaideh is with the Department of Mechanical and Mechatronics Engineering, Memorial University, St. John's, NL A1B 3X5, Canada. maljanaideh@mun.ca. Also, he is with the Department of Mathematics, Czech Technical University, Thákurova 7, 166 29 Praha 6, Czech Republic, and the School of Engineering, Guelph, Guelph, ON, Canada. email: maljanai@uoguelp.ca.

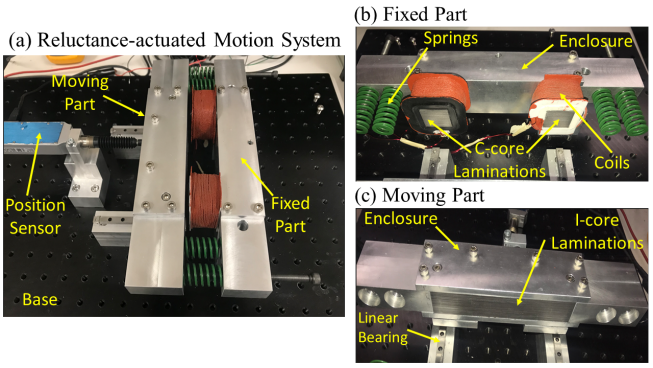

Fig. 1: The proposed design of the reluctance-actuator motion system (RAMS) (a) view of the proposed design; (b) the components of the fixed part (stator); and (c) the components of the moving part (mover).

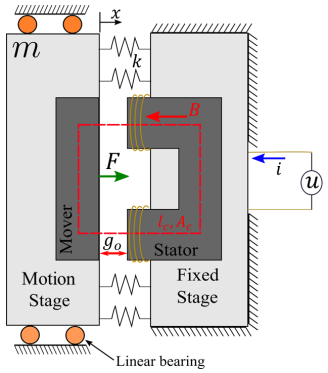

Fig. 2: Schematic diagram of the reluctance-actuated motion system.

measuring or estimating the fast states in the system.

- Design an extended-high gain observer that uses the measured displacement to estimate the slow states in the system and the unknown force effect on the slow dynamic due to the error of the feedforward controller.

II. RELUCTANCE-ACTUATED MOTION SYSTEM

Figure 1(a) illustrates the top view of the proposed reluctance-actuated motion system (RAMS). The system comprises a reluctance actuator attached to a moving stage, which includes linear slide bearings and a preload mechanism as a compression spring. The actuator has a fixed stator comprising C-core laminations and a mover of I-core laminations installed in the moving stage. The magnetic flux generated by the coil in the C-core creates an attractive magnetic force in the air gap between the stator and the mover. This force moves the stage toward the stator in the positive direction $x > 0$. The motion of the stage is resisted by the compression springs, which are set to maintain a nominal air gap between the stator and the mover.

A. Proposed Design

The reluctance actuator utilized in the experiments involved C-core and I-core Nonoriented Electrical Steel (M-19) laminations with a width of 0.35 mm stacked together to achieve a cross-section area of 25×25 mm^2. The excitation coil included two coils on each limb of the C-core with $N = 400$ turns. The fixed stator of the reluctance actuator and the motion stage, represented by the I-core, were implemented in an Aluminum enclosure. The motion stage, weighing approximately $m = 1.65$ kg, was guided by two linear slide bearings, enabling linear motion in the x-axis. Two compression springs (ISO D DIE SPRING) with a total stiffness of about 100 N/mm were utilized to restrict the magnetic force generated and return the motion stage to its initial position. The four springs were also set up to attain a nominal air gap of 2.5 mm, permitting a displacement range of $[0,\ 2]$ mm in the x-direction. Figures 1 (b) and (c) show the components of the fixed part and the moving part, respectively.

B. Dynamic Modeling and problem formulation

Figure 2 depicts the reluctance-actuated motion system, which shows that the actuator's mover is connected to the motion system's stage. During the motion, the air gap g changes continuously with the position x, and it is given by $g = g_o - x$, where g_o represents the nominal air gap when the position is at zero. The interaction among electrical, magnetic, and mechanical behavior is captured by the electromechanical model that is formulated for this system.

To derive the dynamic model of the RAMS, the displacement $x_1 = x$, the velocity $x_2 = \dot{x}$, and the magnetic flux $\xi = B$ is defined as the system's states. Accordingly, the dynamic model of the RAMS can be formulated as [15]

$$\dot{x}_1 = x_2, \tag{1}$$

$$\dot{x}_2 = -\frac{k}{m}x_1 - \frac{b}{m}x_2 + \frac{1}{m}F, \tag{2}$$

$$\dot{\xi} = -\frac{2R}{\mu_o N^2 \mathcal{A}_c}(g_o - x_1)\xi - \frac{lc}{N^2 \mathcal{A}_c}\Psi_h + \frac{1}{N\mathcal{A}_c}u, \tag{3}$$

$$F = \frac{\mathcal{A}_c}{\mu_o}\xi^2, \tag{4}$$

$$y = x_1, \tag{5}$$

where y is the measured output displacement, u is the control input, and Ψ_h is an unknown bounded nonlinear function that presents the magnetic hysteresis of the ferromagnetic material.

Practically, a well-designed reluctance actuator allows selecting the parameters $\mathcal{A}_c$ and N such as the constant $\varepsilon \triangleq \frac{\mu_o \mathcal{A}_c}{N}$ is a small that can be neglected. Then, following the singular perturbation method [11], the RAMS model can be represented in the standard form as

$$\dot{x}_1 = x_2, \tag{6}$$

$$\dot{x}_2 = -\frac{k}{m}x_1 - \frac{b}{m}x_2 + \frac{1}{m}F, \tag{7}$$

$$\varepsilon\dot{\xi} = -\frac{2R}{N^3}(g_o - x_1)\xi + \rho\Psi_h + \frac{\mu_o}{N^2}u, , \tag{8}$$

$$y = x_1, \tag{9}$$

where $\rho = -\frac{l_c \mu_o}{N^3}$ is a constant based on the system parameters.

It can be observed that the RAMS dynamic model evolves in two-time scales, where $x_1,\ x_2$ are the slow states, and ξ is the fast state. The objective is to design a controller so that $y(t) = x_1(t)$ tracks a desired reference signal $r(t)$, which is assumed to be sufficiently smooth and bounded with bounded derivatives.

III. COMPOSITE CONTROL APPROACH

To address the control design problem for the singularly perturbed system, we propose a two-time scale approach, dividing the problem into slow and fast subproblems. The fast dynamic is handled using feedforward control to achieve the desired signal ξ_d. In contrast, the slow dynamics are stabilized through state feedback control to minimize the tracking error between the output $y = x_1$ and the desired motion profile r, even in the presence of unknown errors caused by feedforward compensation. It's important to note that our proposed composite control approach differs from the composite control proposed in previous works, such as [11], [16], as it doesn't require the measurement of the fast state ξ.

A. Feedforward Control Design

The slow subsystem of the system (6)-(8) is obtained by setting $\varepsilon = 0$ in (8) as

$$\dot{x}_1 = x_2, \tag{10}$$

$$\dot{x}_2 = -\frac{k}{m}x_1 - \frac{b}{m}x_2 + \frac{1}{m}F, \tag{11}$$

$$0 = -\frac{2R}{N^3}(g_o - x_1)\xi + \rho\Psi_h + \frac{\mu_o}{N^2}u. \tag{12}$$

Now, we consider a feedforward controller designed to achieve the tracking performance of the fast dynamic, such as the state ξ following a desired flux ξ_d. The feedforward control law can be expressed using the reduced system (12) as

$$u_{ff} = \frac{2R}{N\mu_o}(g_o - x_1)\xi_d, \tag{13}$$

where ξ_d is the input of the feedforward controller. The desired flux ξ_d is calculated based on a desired force F_d as

$$\xi_d = \sqrt{\frac{\mu_o}{\mathcal{A}_c}F_d}, \tag{14}$$

Applying the feedforward control law u_{ff} into the system (6)-(8), we have

$$\dot{x}_1 = x_2, \tag{15}$$

$$\dot{x}_2 = -\frac{k}{m}x_1 - \frac{b}{m}x_2 + \frac{1}{m}F, \tag{16}$$

$$\varepsilon\dot{\xi} = -\frac{2R}{N^3}(g_o - x_1)(\xi - \xi_d) + \rho\Psi_h, \tag{17}$$

Consider the error due to the feedforward controller being defined by $e_f = \xi - \xi_d$; thus, the system (6)-(8) with the feedforward control law (13) can be expressed as

$$\dot{x}_1 = x_2, \tag{18}$$

$$\dot{x}_2 = -\frac{k}{m}x_1 - \frac{b}{m}x_2 + \frac{1}{m}F, \tag{19}$$

$$\varepsilon\dot{e}_f = -\frac{2R}{N^3}(g_o - x_1)e_f + \rho\Psi_h - \varepsilon\dot{\xi}_d. \tag{20}$$

According to (4), the input force F for the system (18)-(19) can be expressed as

$$\begin{aligned} F =& \frac{\mathcal{A}_c}{\mu_o}\xi^2 = \frac{\mathcal{A}_c}{\mu_o}(\xi_d + e_f)^2, \\ =& \frac{\mathcal{A}_c}{\mu_o}\xi_d^2 + \frac{\mathcal{A}_c}{\mu_o}\left(2\xi_d + e_f\right)e_f, \end{aligned} \tag{21}$$

Using (14) and (21), the system (18)-(20) is rewritten as

$$\dot{x}_1 = x_2, \tag{22}$$

$$\dot{x}_2 = -\frac{k}{m}x_1 - \frac{b}{m}x_2 + \frac{1}{m}F_d + \delta_{ff}, \tag{23}$$

$$\varepsilon\dot{e}_f = -\frac{2R}{N^3}(g_o - x_1)e_f + \rho\Psi_h - \varepsilon\dot{\xi}_d. \tag{24}$$

where $\delta_{ff} \triangleq \frac{\mathcal{A}_c}{\mu_o m}\left(2\xi_d + e_f\right)e_f$ is an unknown function that represents the force effect on the motion system due to the unknown feedforward error e_f.

Now, the slow subsystem of the system (22)-(24) is obtained by setting $\varepsilon = 0$ in (24) as

$$\dot{x}_1 = x_2, \tag{25}$$

$$\dot{x}_2 = -\frac{k}{m}x_1 - \frac{b}{m}x_2 + \frac{1}{m}F_d + \delta_{ff}, \tag{26}$$

$$e_f = \frac{\rho N^3}{2R(g_o - x_1)}\Psi_h. \tag{27}$$

where $g_o - x_1 > 0$ from a practical point of view based on the proposed design of the RAMS. The system (27) indicates that the feedforward error e_f depends on the unknown nonlinearities Ψ_h.

B. Full-State Feedback Control

Toward achieving the tracking goal, we introduce the error variables as

$$e_1 = x_1 - r, \quad e_2 = x_2 - w, \tag{28}$$

where we recall that r is the desired reference position with bounded derivatives, and w is a desired signal selected as

$$w = -k_1 e_1 + \dot{r}, \tag{29}$$

with k_1 being a positive parameter to be designed. In view of this change of variable, the system (18)-(20) is written as

$$\dot{e}_1 = -k_1 e_1 + e_2, \tag{30}$$

$$\dot{e}_2 = -\frac{k}{m}(e_1 + r) - \frac{b}{m}(e_2 + w) - \dot{w} + \frac{1}{m}F_d + \delta_{ff}, \tag{31}$$

$$\varepsilon\dot{e}_f = -\frac{2R}{N^3}\left(g_o - (e_1 + r)\right)e_f + \rho\Psi_h - \varepsilon\dot{\xi}_d. \tag{32}$$

To achieve the desired tracking objective, the goal is to ensure exponential stability at the system's origin described

by equations (30)-(31) through the design of a suitable state feedback control ξ_d. For this purpose, consider a smooth and positive definite Lyapunov function as $V_a = \frac{1}{2}e_1^2 + \frac{1}{2}e_2^2$, where the derivative of V_a along the system (30)-(31) is given as

$$\dot{V}_a = -k_1 e_1^2 + e_1 e_2 + e_2\left(-\frac{k}{m}(e_1+r) - \frac{b}{m}(e_2+w) - \dot{w} + \gamma(\xi_d+e_f)^2\right), \tag{33}$$

the the input ξ_d can be selected as

$$F_d \triangleq \Gamma(e_1, e_2, e_f, \sigma, w), \tag{34}$$

$$\Gamma = m\left(-k_2 e_2 + \frac{k}{m}(e_1+r) - \sigma + \dot{w}\right), \tag{35}$$

where $\dot{w} = -k_1\dot{e}_1 + \ddot{r}$, k_2 is a positive parameters to be designed, and σ is defined as

$$\sigma = -\frac{b}{m}(e_2+w) + \delta_{ff}. \tag{36}$$

The function σ is utilized to capture the unknown dynamics of the system arising from the unknown damping coefficient b and the unknown force generated by the feedforward controller. Moreover, this function can be estimated using an extended high-gain observer (EHGO), as demonstrated later, and can thus be utilized in the feedback controller.

With the selection of F_d as (35), the derivative of V_a satisfies

$$\dot{V}_a = e_1\dot{e}_1 + e_2\dot{e}_2 = -e_a^T Q_a e_a, \leq -\lambda_{\min}(Q_a)\|e_a\|^2. \tag{37}$$

where $e_a = \begin{bmatrix} e_1 & e_2 \end{bmatrix}^T$ and $Q_a = \begin{bmatrix} k_1 & 0.5 \\ 0.5 & k_2 \end{bmatrix}$ is a positive definite matrix.

Thus, the system (30)-(32) with the feedforward control (13) and state feedback control (35) is expressed as

$$\dot{e}_a = A_1 e_a, \tag{38}$$

$$\varepsilon\dot{e}_f = -\frac{2R}{N^3}\left(g_o - (e_1+r)\right)e_f + \rho\Psi_h - \varepsilon\dot{\xi}_d, \tag{39}$$

where $A_1 = \begin{bmatrix} -k_1 & 1 \\ 0 & -k_2 \end{bmatrix}$ is a Hurwitz matrix by selecting k_1 and k_2. The closed-loop system (38)-(39) is in the standard singularly perturbed form with a two-time scale structure. The slow variable is $e_a(t)$, and the fast variable is $e_f(t)$. By setting $\varepsilon = 0$ in (39), the system (38) has an exponential stable equilibrium point at $e_a = 0$, and the reduced system (39) has an equilibrium point at $e_f = \frac{\rho N^3}{2R(g_o - r)}\Psi_h$.

Assumption 1. *The nonlinear function Ψ_h captures the magnetic hysteresis nonlinearity of the reluctance actuator, which depends on the system's magnetic flux ξ. Specifically, $\psi_h = 0$ when $\xi = 0$. Additionally, the hysteresis is physically limited by the magnetic properties of the ferromagnetic material. Hence, the function Ψ_h is assumed to be bounded with $\|\Psi_h\|$.*

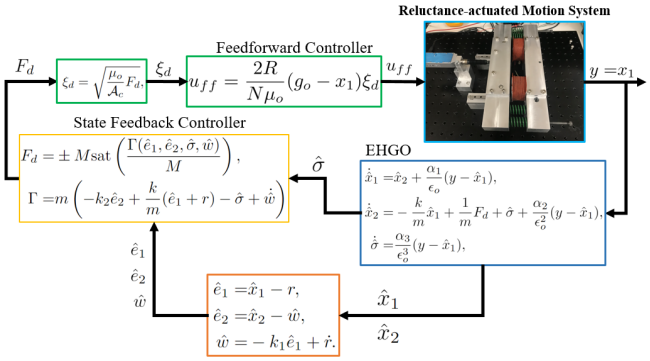

Fig. 3: Block diagram representation of the proposed control approach for the reluctance-actuated motion system.

IV. Output Feedback Control

The previous section presented the controller design assuming all dynamic states for the controller and knowledge of the nonlinear function σ. However, this assumption requires measurements of all these signals, which is impractical and requires additional sensing devices. This section uses an extended high-gain observer (EHGO) to estimate the dynamics and the function σ in (36) that represents the unknown force error due to the feedforward controller using the feedback measurements of the position only. Then, it is combined with the proposed controller to solve the output feedback control problem.

A. Extended High Gain Observer

The concept of the Extended High Gain Observer (EHGO) is used to estimate the states and the unknown hysteresis nonlinearities of the nonlinear dynamic systems [17]. The proposed observer is a structured cascade of observers with two EHGOs, where the first EHGO is designed to estimate the states x_1, x_2, and the function σ. The EHGO is formulated as

$$\dot{\hat{x}}_1 = \hat{x}_2 + \frac{\alpha_1}{\epsilon_o}(y - \hat{x}_1), \tag{40}$$

$$\dot{\hat{x}}_2 = -\frac{k}{m}\hat{x}_1 + \frac{1}{m}F_d + \hat{\sigma} + \frac{\alpha_2}{\epsilon_o^2}(y - \hat{x}_1), \tag{41}$$

$$\dot{\hat{\sigma}} = \frac{\alpha_3}{\epsilon_o^3}(y - \hat{x}_1), \tag{42}$$

where $\epsilon_o > 0$ is a small parameter to be designed, and α_1, α_2, and α_3, are chosen such that the polynomial $s^3 + \alpha_1 s^2 + \alpha_2 s + \alpha_3 = 0$ is Hurwitz. The error dynamic is given by

$$\hat{e}_1 = \hat{x}_1 - r, \quad \hat{e}_2 = \hat{x}_2 - \hat{w}, \quad \hat{w} = -k_1\hat{e}_1 + \dot{r}. \tag{43}$$

B. Output Feedback Control

High-gain observers are known to have the ability to recover performance of any stabilizing state-feedback controller [18]–[22]. This property is beneficial in shaping the transient performance of the closed-loop system. In what follows, we will combine the state feedback controller with the proposed observer to solve the output-feedback control

problem. Accordingly, we use the output-feedback control using the estimated states as

$$F_d = \pm M \text{sat}\left(\frac{\Gamma(\hat{e}_1, \hat{e}_2, \hat{\sigma}, \hat{w})}{M}\right), \tag{44}$$

where the control law Γ is defined in (35) and sat(.) is the saturation function which is used to protect the system from peaking in the observer's transient response [23]. The saturation limit M is chosen to include the set defining the states under state feedback control. In practice, the value of M is selected based on the maximum force of the mechanical system. Figure 3 represents the closed-loop representation of the proposed output feedback control approach with EHGO.

To analyze the performance of the closed-loop system, consider the scaled estimation errors

$$\chi_1 = \frac{x_1 - \hat{x}_1}{\epsilon_o^2}, \quad \chi_2 = \frac{x_2 - \hat{x}_2}{\epsilon_o}, \quad \chi_3 = \sigma - \hat{\sigma}. \tag{45}$$

Using the scaled error, the closed-loop system under the output feedback can be expressed by the system (38)-(39) and the observer (40)-(42) as

$$\dot{e}_a = A_1 e_a, \tag{46}$$

$$\epsilon_o \dot{\chi} = \Lambda_1 \chi + \epsilon_o \left[B_1 \Delta_1 + B_2 \dot{\sigma}\right], \tag{47}$$

$$\varepsilon \dot{e}_f = -\frac{2R}{N^3}\left(g_o - (e_1 + r)\right) e_f + \rho \Psi_h - \varepsilon \dot{\xi}_d, \tag{48}$$

where $\Lambda_1 = \begin{bmatrix} -\alpha_1 & 1 & 0 \\ -\alpha_2 & 0 & 1 \\ -\alpha_3 & 0 & 0 \end{bmatrix}$, $B_1 = \begin{bmatrix} 0 \\ 1 \\ 0 \end{bmatrix}$, $B_2 = \begin{bmatrix} 0 \\ 0 \\ 1 \end{bmatrix}$ and $\Delta_1 = -\frac{k}{m}\epsilon_o \chi_1$. Equations (46)-(48) are in the standard singularly perturbed form with a three-time scale structure. The slow variable of this structure is $e_a(t)$ and the fast variables are $(e_f(t), \chi(t))$, moreover, $e_f(t)$ is faster than $\chi(t)$. Let $(\chi) \in Z \subset \mathbb{R}^3$ where Z is a compact set.

V. EXPERIMENTAL VERIFICATION

The experimental tests of the RAMS are carried out for verification of the proposed control approach. In this test, we consider a step response and tracking of a sinusoidal motion profile.

A. Step response:

For this experimental setup, a step signal with an amplitude of 1mm was chosen as the desired reference signal. The tracking performance of the measured displacement $x(t)$ is shown in Figure 4(a), which indicates that the proposed controller achieves the desired signal with an error of approximately 19.85 μm. The feedforward voltage $u_{ff}(t)$ of the control law (13) and the desired force F_d of the feedback control (35) are illustrated in Figure 4(b)(a). The figure depicts that a high voltage is required at time zero to initiate motion. The steady-state value of the desired force is approximately $F_d = 46.26$ N, and the steady-state value of the voltage is around $u_{ff} = 5.32$ V.

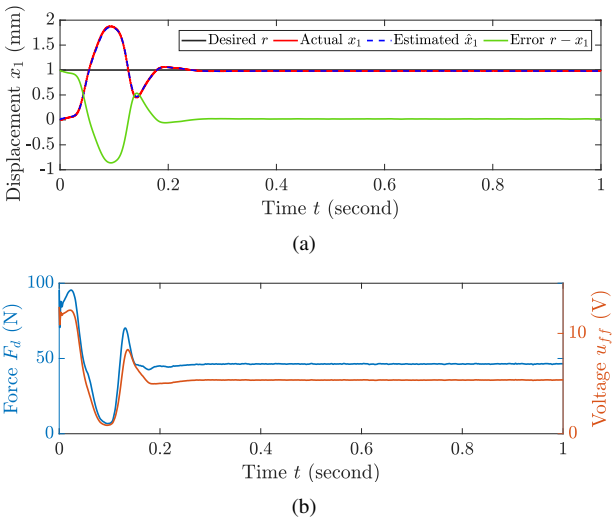

Fig. 4: Step response of the RAMS using the proposed control approach (a) tracking performance of the displacement x_1(mm); and (b) the desired force F_d (N) and the feedforward voltage u_{ff} (V).

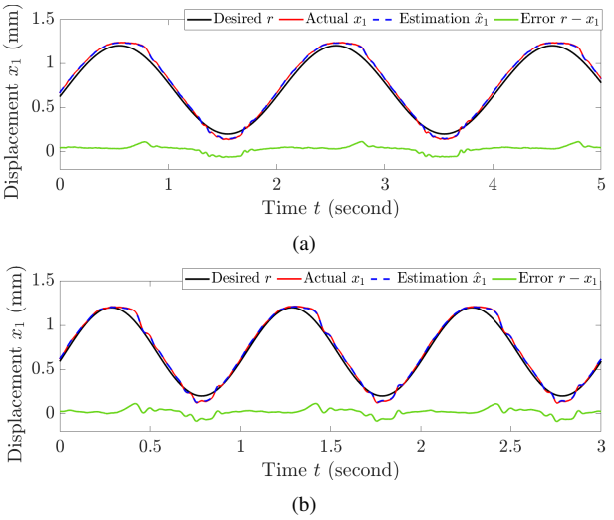

Fig. 5: Tracking performance of the displacement x_1(mm) to a desired sinusoidal motion profile as $r(t) = 0.5\sin(2\pi f t) + 0.7$ for (a) frequency $f = 0.5$ Hz; and (b) frequency $f = 1$ Hz.

B. Sinusoidal motion profile:

In this experiment, a sinusoidal motion profile with two different frequencies is designed as $r(t) = 0.5\sin(2\pi f t) + 0.7$mm, where f takes on values of 0.5Hz, and 1Hz. The tracking performance of the measured displacement $x(t)$ for the selected frequencies is presented in Figure 5 with the tracking error $e(t) = r(t) - x(t)$. It can be observed that the proposed controller can achieve the desired signal with a bounded error of $[-84, 114](\mu$m). Figure 6 shows the output force F_d of the state feedback controller and the feedforward voltage u_{ff} as a function of time.

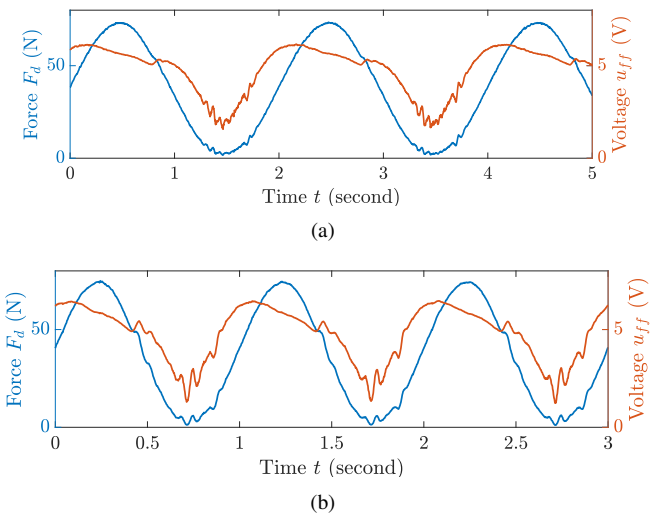

Fig. 6: The desired force F_d from the state feedback control (35) and the voltage u_{ff} from the feedforward control (13) for a desired reference $r(t) = 0.5\sin(2\pi ft) + 0.7$ for (a) frequency $f = 0.5$ Hz; and (b) frequency $f = 1$ Hz.

VI. CONCLUSION

Using a singular perturbation approach, the paper presents a novel composite control strategy for a reluctance-actuated motion system (RAMS) with unknown nonlinearities. The proposed approach formulates the dynamic model of the RAMS as a two-time-scale model. Firstly, a feedforward controller is designed based on a reduced system to achieve a tracking objective of the fast dynamics. Next, a full-state feedback controller is designed to stabilize the slow dynamics and achieve a desired output displacement while considering all states and unknown forces due to the available feedforward controller. However, since the states and the unknown dynamics may not be available for the controller, an extended high-gain observer (EHGO) is designed based on the slow dynamics to estimate the slow states and unknown nonlinear function using only the measured output. Finally, an output feedback control is proposed by integrating the state feedback with the EHGO. The effectiveness of the proposed approach is demonstrated through experimental results, which show that it can achieve the desired tracking motion profile and reduce tracking errors. Future work will generalize the proposed control approach for a two-time scale dynamic model in different mechatronics applications.

REFERENCES

[1] M. Steinbuch, T. Oomen, and H. Vermeulen, "Motion control, mechatronics design, and moore's law," *IEEJ Journal of Industry Applications*, vol. 11, no. 2, pp. 245–255, 2022.

[2] M. Heertjes, H. Butler, N. Dirkx, S. van der Meulen, R. Ahlawat, K. O'Brien, J. Simonelli, K. Teng, and Y. Zhao, "Control of wafer scanners: Methods and developments," in *2020 American Control Conference (ACC)*. IEEE, 2020, pp. 3686–3703.

[3] Y. Wei, V. Nguyen, and W. Kim, "A 3-D printed halbach-cylinder motor with self-position sensing for precision motions," *IEEE/ASME Transactions on Mechatronics*, vol. 27, pp. 1489–1497, 2022.

[4] A. Katalenic, H. Butler, and P. Van Den Bosch, "High-precision force control of short-stroke reluctance actuators with an air gap observer," *IEEE/ASME Transactions on Mechatronics*, vol. 21, pp. 2431–2439, 2016.

[5] I. MacKenzie and D. Trumper, "Real-time hysteresis modeling of a reluctance actuator using a sheared-hysteresis-model observer," *IEEE/ASME Transactions on Mechatronics*, vol. 21, pp. 4–16, 2016.

[6] Y. Xu, X. Li, X. Yang, Z. Yang, L. Wu, and Q. Chen, "A two-stage model for rate-dependent inverse hysteresis in reluctance actuators," *Mechanical Systems and Signal Processing*, vol. 135, pp. 1–18, 2020.

[7] X. Zhang, L. Lai, P. Li, and L. Zhu, "Data-driven fractional order feedback and model-less feedforward control of a xy reluctance-actuated micropositioning stage," *Review of Scientific Instruments*, vol. 93, no. 11, p. 115002, 2022.

[8] E. Moya-Lasheras, E. Ramirez-Laboreo, and C. Sagues, "Probability-based optimal control design for soft landing of short-stroke actuators," *IEEE Transactions on Control Systems Technology*, vol. 28, no. 5, pp. 1956–1963, 2019.

[9] F. Cigarini, S. Ito, S. Troppmair, and G. Schitter, "Comparative finite element analysis of a voice coil actuator and a hybrid reluctance actuator," *IEEJ Journal of Industry Applications*, vol. 8, pp. 192–199, 2019.

[10] X. Zhang, L. Lai, L. Zhang, and L. Zhu, "Hysteresis and magnetic flux leakage of long stroke micro/nanopositioning electromagnetic actuator based on maxwell normal stress," *Precision Engineering*, vol. 75, pp. 1–11, 2022.

[11] P. Kokotović, H. K. Khalil, and J. O'reilly, *Singular perturbation methods in control: analysis and design*. SIAM, 1999.

[12] P. Li, L. Wang, B. Zhong, and M. Zhang, "Linear active disturbance rejection control for two-mass systems via singular perturbation approach," *IEEE Transactions on Industrial Informatics*, vol. 18, no. 5, pp. 3022–3032, 2021.

[13] T. Braun, J. Reuter, and J. Rudolph, "A singular perturbation approach to nonlinear observer design with an application to electromagnetic actuators," *International Journal of Control*, vol. 93, no. 9, pp. 2015–2028, 2020.

[14] R. Mallik, B. Majmunović, S. Dutta, G.-S. Seo, D. Maksimović, and B. Johnson, "Control design of series-connected pv-powered grid-forming converters via singular perturbation," *IEEE Transactions on Power Electronics*, 2022.

[15] M. Al Saaideh, A. M. Boker, and M. Al Janaideh, "Output-feedback control of electromagnetic actuated micropositioning system with uncertain nonlinearities and unknown gap variation," in *2022 IEEE 61st Conference on Decision and Control (CDC)*, 2022, pp. 2481–2486.

[16] A. Saberi and H. Khalil, "Stabilization and regulation of nonlinear singularly perturbed systems–composite control," *IEEE Transactions on Automatic Control*, vol. 30, no. 8, pp. 739–747, 1985.

[17] H. Khalil, "Extended high-gain observers as disturbance estimators," *SICE Journal of Control, Measurement, and System Integration*, vol. 10, no. 3, pp. 125–134, 2017.

[18] A. M. Boker and H. K. Khalil, "Control of flexible joint manipulators using only motor position feedback: A separation principle approach," in *Proceeding of the 52nd IEEE Conference on Decision and Control*, 2013, pp. 244–249.

[19] H. Khalil, "High-gain observers in feedback control: Application to permanent magnet synchronous motors," *IEEE Control Systems Magazine*, vol. 37, pp. 25–41, 2017.

[20] M. Al Janaideh, A. Boker, and M. Rakotondrabe, "Output-feedback control of precision motion systems with uncertain nonlinearities," *Mechanical Systems and Signal Processing*, vol. 153, pp. 1–20, 2021.

[21] A. Boker and H. Khalil, "Nonlinear observers comprising high-gain observers and extended kalman filters," *Automatica*, vol. 49, pp. 3583–3590, 2013.

[22] ——, "Semi-global output feedback stabilization of non-minimum phase nonlinear systems," *IEEE Transactions on Automatic Control*, vol. 62, pp. 4005–4010, 2016.

[23] F. Esfandiari and H. Khalil, "Output feedback stabilization of fully linearizable systems," *International Journal of control*, vol. 56, pp. 1007–1037, 1992.